

pubs.acs.org/jcim Article

Analysis of the First Ion Coordination Sphere: A Toolkit to Analyze the Coordination Sphere of Ions

Stuart J. McElhany, Thomas J. Summers, Richard C. Shiery, and David C. Cantu*



Cite This: J. Chem. Inf. Model. 2023, 63, 2699-2706



Read Online

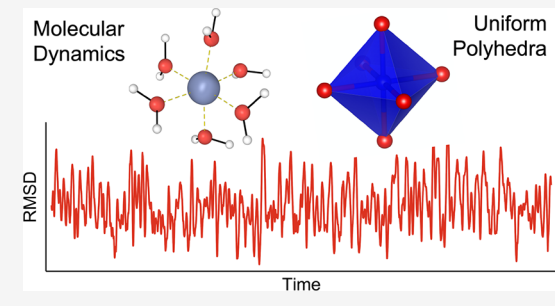
ACCESS I

Metrics & More

Article Recommendations

s Supporting Information

ABSTRACT: Rapid and accurate approaches to characterizing the coordination structure of an ion are important for designing ligands and quantifying structure—property trends. Here, we introduce AFICS (Analysis of the First Ion Coordination Sphere), a tool written in Python 3 for analyzing the structural and geometric features of the first coordination sphere of an ion over the course of molecular dynamics simulations. The principal feature of AFICS is its ability to quantify the distortion a coordination geometry undergoes compared to uniform polyhedra. This work applies the toolkit to analyze molecular dynamics simulations of the well-defined coordination structure of aqueous Cr³⁺ along with the more ambiguous structure of aqueous Eu³⁺ chelated to ethylenediaminetetraacetic



acid. The tool is targeted for analyzing ions with fluxional or irregular coordination structures (e.g., solution structures of *f*-block elements) but is generalized such that it may be applied to other systems.

INTRODUCTION

Cations in solution form coordination bonds with surrounding molecules, resulting in a solution coordination structure dependent on the ion, solvent, counterion, and ligand molecules present. Solutions have more degrees of freedom (vibrational, rotational, and translational) than crystals or soft materials, resulting in experimentally measured solution structures that are an average of multiple conformations that can vary greatly due to the disorder of the system. Metrics such as Debye–Waller factors quantify disorder; however, to describe the molecular conformations that correspond to disordered structures, molecular modeling is often necessary. ^{1–3}

Aqueous solutions of ions (namely alkali, alkaline earth, transition, lanthanide, and actinide elements) have been widely studied compared to other solvents. Different ions exhibit distinct properties and behavior, and the structure of hydrated ions widely varies based on their electronic configuration. ⁴ The complexity of their structure further increases if ligands and counterions also coordinate with the ion. While electronic structure calculations can obtain the optimized conformation of the first coordination sphere of an ion and describe its shape,⁵⁻⁸ they are unable to quantify the disorder in the structure in solution. To resolve this, molecular dynamics (MD) simulations with periodic boundary conditions may be used to simulate the solution structure of an ion, whether based on density functional theory or a parametrized classical force field. 9-14 It is possible to resolve the elusive structures of ions in solution with X-ray absorption spectroscopy measurements¹⁵⁻²¹ as well as by combining X-ray absorption

spectroscopy measurements with MD simulations and/or electronic structure calculations. $^{22-37}$

Ensemble structures from MD simulations can be used to determine the multiple conformations of the first coordination sphere of an ion in solution. The radial distribution function (RDF) is a histogram of all ion—atom distances over all molecular conformations of the simulation. The distance of the first peak of the RDF quantifies the average ion—atom bond lengths in the first sphere, and the coordination number (CN) of the first sphere of the ion can be calculated from the integral of the first peak in the RDF. The angle distribution function (ADF) is a histogram of all atom—ion—atom bonds in the first coordination sphere, and it can be used to determine the dominant shape of an ion in solution, such as a square antiprism shape for the Lu³+ aqua ion. By combining distance and angle distribution plots, molecular geometries of the ion coordination sphere in solution can be identified. 14

One way to quantify how much a solution structure varies from its dominant, or favored, shape (geometry) is to calculate the root-mean-square deviation (RMSD) of the solution structures to an ideal polyhedron, as was recently demonstrated in our works characterizing solution structures of Ln³⁺ aqua ions at different temperatures. 35,36 RMSD measures the

Received: February 24, 2023 Published: April 21, 2023





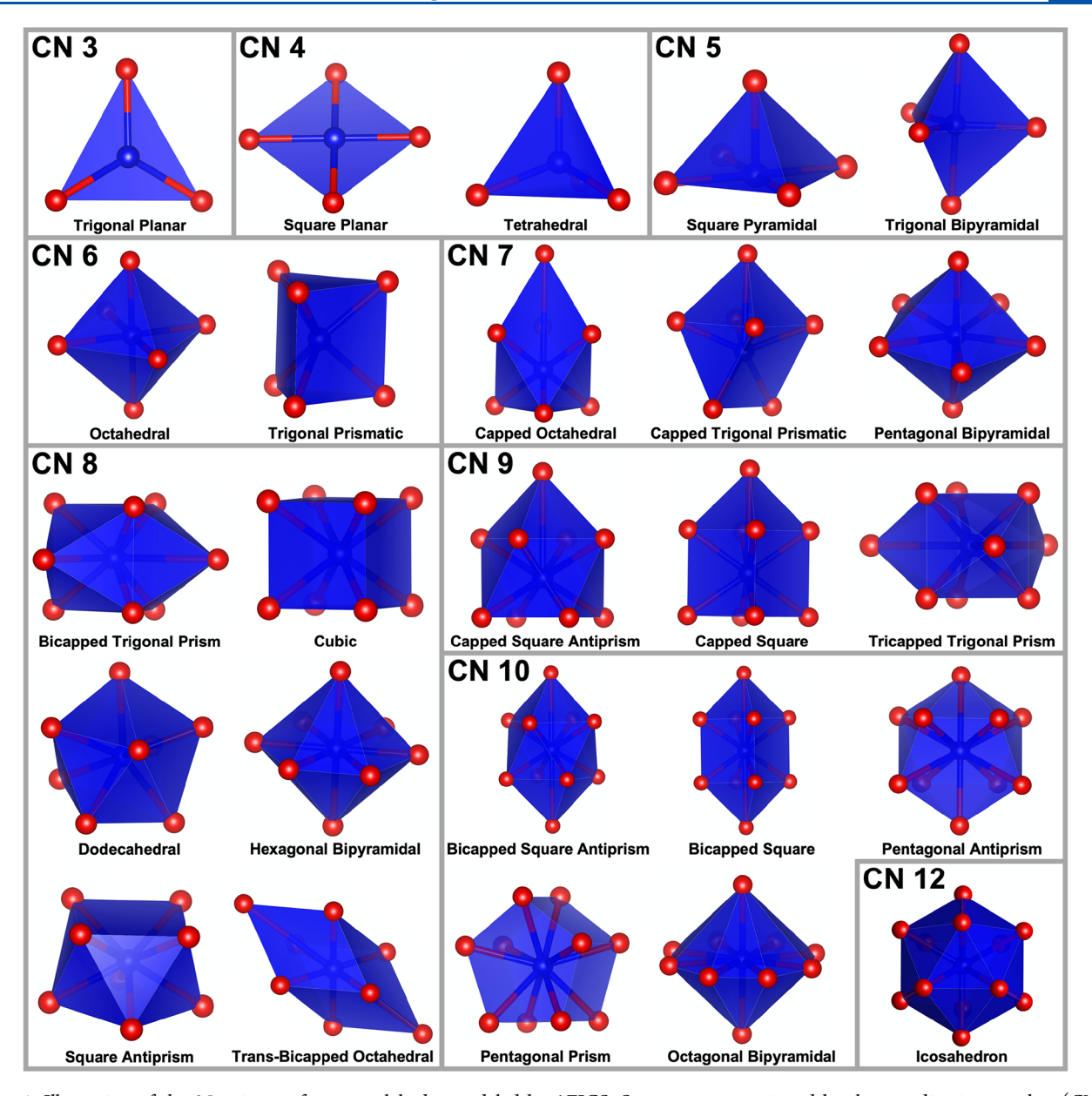


Figure 1. Illustration of the 25 unique reference polyhedra modeled by AFICS. Structures are sectioned by the coordination number (CN) of atomic vertices (red spheres) to the central ion (blue sphere). The ion–vertex distances in the reference polyhedra are based on the maximum of the first g(r) peak identified in the RDF to match the size of reference geometries to the size of the first coordination sphere.

difference in positions between corresponding atoms of two different structures. RMSDs have been used in structural biochemistry to quantify numerous properties, such as quantifying the similarity between protein structures and reporting the accuracy of ligand docking predictions. Structures in inorganic chemistry have been mostly studied in the solid or crystal phases, and due to their static nature and symmetric arrangements, RMSD calculations have been used less frequently to describe inorganic structures. However, in solution, RMSD may serve to quantify the disorder of the first coordination sphere.

To describe the RMSD calculations to ideal geometries, we focus on the solution structure of an aqua ion and an ion—ligand complex in water; however, RMSD calculations can also be done with ions in non-aqueous solvents. Ligand complexation will change the structure of the first coordination sphere, for example, in lanthanide—ligand complexes, 44–50 and RMSD

calculations can be used to quantify how the structure changes. A specific example: binding with EDTA^{4–} will change the preferred geometry of the ${\rm Lu^{3+}}$ ion from square antiprismatic in water to dodecahedral. Ions are also found in proteins and in enzyme active sites, $^{52-58}$ and RMSD calculations could also be used to characterize the first coordination sphere of ions in proteins and enzymes from MD simulations.

Although this work describes how deviations in the coordination structure of ions can be quantified with RMSDs, mostly in the context of solution coordination chemistry or in soft matter, RMSDs could also be used in the solid state. Different approaches have been developed to quantify distortions of coordination spheres in the solid state, mostly for transition elements. For example, OctaDist quantifies deviations from an ideal octahedral geometry using average metal—ligand distances as well as stretching, angular, and torsional distortions. ⁵⁹ When coordination complexes

transition from one geometry to another, ideal geometries are distorted. Quantifying transition distortions in terms of continuous shapes can help identify minimum distortion paths. $^{60-62}$

To streamline the aforementioned analyses, we developed AFICS, a tool for the Analysis of the First Ion Coordination Sphere. Given the atomic coordinates from molecular simulation, AFICS calculates the RDF, CN, ADF, and RMSD to the ideal geometries of the CN of the ion. While many other programs and toolkits are available to compute RDFs and CNs, the usefulness of AFICS lies in its capability of quantifying the geometric disorder (RMSD) of the first coordination sphere of an ion from ideal geometries. This manuscript details the design of the AFICS toolkit and demonstrates its application toward analyzing MD simulations of two model structures: the Cr³⁺ aquo complex and aqueous Eu³⁺ chelated by ethylenediaminetetraacetic acid (EDTA).

METHODOLOGY

Calculation of Distribution Functions. The radial distribution function measures the average distribution of atoms around a central reference atom as a function of distance from the reference. Users first identify the central reference ion and then identify which element(s) surrounding the reference should be used in the RDF measurement. As the RDF guides identification of the ion coordination number and geometric RMSD, users should only specify elements that directly coordinate the ion over the course of the MD trajectory (e.g., only the oxygen atoms for an ion-aquo complex). For each frame in the MD trajectory, the distance between the reference and all specified element types is computed, and the count and distances of atoms within 6 Å are aggregated into a histogram representing the first coordination sphere of the ion. The RDF is calculated from this data using the equation

$$g(r) = \frac{1}{\frac{4}{3}\pi \cdot B_i \cdot r} \cdot \frac{1}{4\pi \cdot (\text{binNum} + 1)^2 \cdot \text{bin}^3}$$
(1)

where B_i is the count of atoms at a given distance r from the ion, bin is the bin width, and binNum is one iteration of the range of the maximum value for r (6 Å) divided by the bin. The integral of g(r) up to the first shell threshold distance measures the coordination number (CN) of the first shell. The threshold of the first shell is identified as the distance where the change in the integral of g(r) is less than 0.002 for at least two bin width distances. The CN is calculated from the RDF of the whole trajectory, so changes in the CN as a function of trajectory are not tracked. The CN will default to the rounded integer from integrating the first peak of the RDF. Since the g(r) from a trajectory is required for AFICS to calculate a CN, it cannot estimate the CN from geometry only, for example, in the way that the solid angle-based nearest neighbor approach can. 63,64

The angle distribution function (ADF) is similar to the RDF, though it measures the average of the angles formed between pairs of user-defined elements using the central ion as the vertex. For all atom pair combinations of selected elements within 6 Å of the reference ion, the angle formed is computed by the equation

$$angle = arccos \left(\frac{a^2 + b^2 - c^2}{2ab} \right)$$
 (2)

where a and b are the distances from the reference ion to two first sphere atoms and c is the interatomic distance between the two first sphere atoms. All atom—ion—atom angles measured over the course of the MD trajectory are aggregated to yield the ADF histogram.

Calculation of Deviation from Ideal Geometries. For many polyhedra, each of the atomic vertices is equidistant to the central ion (e.g., trigonal planar, octahedral, and cubic). The ideal reference geometries for these polyhedra are constructed so the distance between the central ion and each atomic vertex is equal to the maximum of the first g(r) peak identified in the RDF, which represents the time-averaged distance of the coordinating atoms to the ion. Capped polyhedra (e.g., capped octahedral, capped square, and bicapped square) have more than one ion-vertex distance in their model structures. The ideal reference geometries for these polyhedra are constructed so the average of all ion-vertex distances is equal to the maximum of the first g(r) peak identified in the RDF. The reference geometries that AFICS uses to calculate RMSDs are illustrated in Figure 1, and they include 25 different geometries whose coordination numbers range from 3 to 12.

After creating the reference polyhedra for the appropriate CN of the system, 65-68 each of the reference geometries of the corresponding CN (Figure 1) is superimposed against the first coordination sphere of the ion in the MD trajectory structures to measure their RMSDs over MD timeframes. For each frame in the MD trajectory, each reference polyhedron with the corresponding CN is aligned to best fit the polyhedral vertices to the MD ion sphere atoms. Only the reference polyhedra of the corresponding CN will be aligned for RMSD calculation; however, users can choose a different CN than that identified from the integral of the RDF. For example, if the integral of the RDF is 8.6, then AFICS will set the CN to 9; however, users can change it to 8 and calculate the RMSD to eight-coordinate geometries instead of nine-coordinate geometries. Only the MD frames that have the same CN as that set will be used for the RMSD calculation.

Matching the atoms from the reference polyhedra to those in MD frames is conducted using the Kabsch algorithm that minimizes the RMSD between the geometric points. ⁶⁹ As the Kabsch alignment is fit for given reference-MD atom pairs, all permutations of the reference geometry atom ordering are considered for the first MD structure to ensure that the lowest RMSD alignment is obtained; as repeated permutation operations can become costly, users are able to set how frequently the permutations of the reference ordering are recomputed. The final RMSD between the reference geometry structure and the MD trajectory structure is reported for each MD frame. The RMSD is calculated with the equation

RMSD =
$$\sqrt{\frac{1}{N} \sum_{i=1}^{N} \|a_i - b_i\|^2}$$
 (3)

where N is the number of vertices in the polyhedra that should equal the CN of the system and a and b are the spatial position polyhedral vertices of the reference geometry and spatial positions of the atoms in the first ion coordination sphere in an MD frame. An RMSD of 0 means that the coordination geometry is an exact match to an ideal geometry. AFICS does not assign a preferred geometry, rather it reports RMSD values to all ideal geometries of the set CN; the ideal geometry with

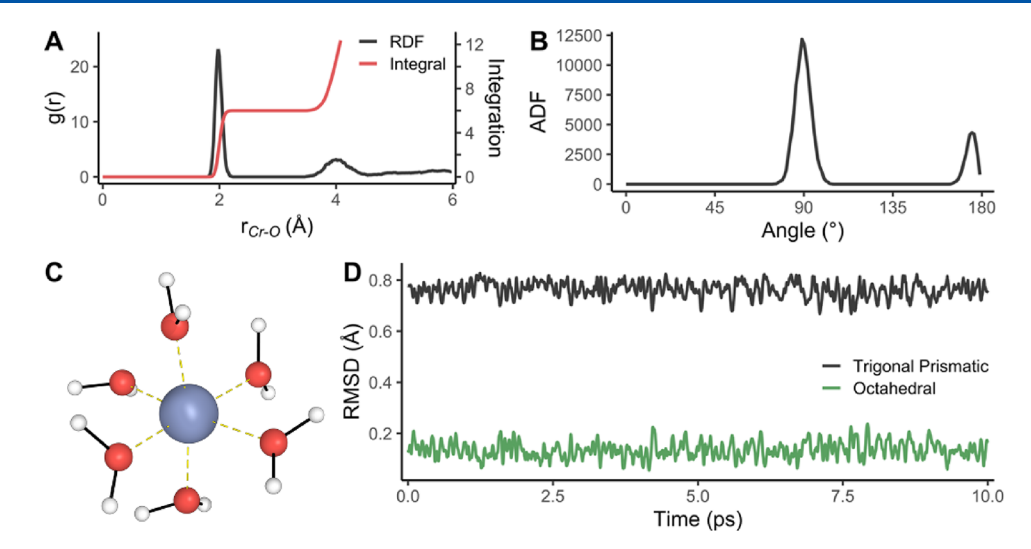


Figure 2. Structural characteristics of the aqueous Cr^{3+} simulation: (A) radial distribution function of Cr-O distances, (B) angle distribution function formed with Cr^{3+} and surrounding waters, (C) ball-and-stick model of the first coordination sphere surrounding Cr^{3+} , and (D) deviation of the first ion coordination sphere structure from ideal polyhedral structures over the MD trajectory.

the lowest RMSD is the one that best describes the coordination structure.

■ IMPLEMENTATION AND APPLICATIONS

The code for the AFICS toolkit is available on GitHub (https://github.com/Cantu-Research-Group/AFICS). To demonstrate AFICS and its usage, we detail its application toward analyzing molecular dynamics (MD) simulations of two model structures: the Cr³⁺ aquo complex and aqueous Eu³⁺ complexed with ethylenediaminetetraacetic acid (EDTA). Example AFICS input files for processing both model simulations are available on GitHub and in the accompanying Supporting Information.

Simulation of Hexaaqua Chromium(III). In aqueous solution, the Cr³⁺ ion is known to have six waters coordinate to the metal in an octahedral geometry. 70-74 The ion complex is fairly acidic and will typically have a coordinated water donate a proton to form $[Cr(H_2O)_5(OH)]^{2+}$, but for this model, we will focus on only the hexaaqua structure. To examine the dynamic structural properties of $[Cr(H_2O)_6]^{3+}$, an *ab initio* molecular dynamics (AIMD) simulation was constructed for Cr3+ (quartet spin state) within a periodic cube (cell length 12.42 Å) containing 64 water molecules (Figure S1). Three chloride ions were added to neutralize the charge of the system, and they are positioned suitably away from the Cr³⁺ ion to prevent substitution with any of the coordinated waters. To accurately replicate bond lengths and geometries, the system was modeled with density functional theory using the Perdew-Burke-Ernzerhof (PBE) functional⁷⁵ as implemented in the CP2K v5.1 program. 76,77 Core electrons were described using Goedecker-Teter-Hutter (GTH) pseudopotentials, while valence electrons were described by a double- ξ valence polarized (DZVP) basis sets.⁷⁹ Long-range electrostatics were accounted for using an auxiliary plane-wave basis set using a 500 Ry cutoff, along with van der Waals interactions using Grimme's D3 corrections with a 6 Å radius cutoff.⁸⁰ The system was simulated in the NVT ensemble at 300 K with a timestep of 1 fs and until at least 10 ps of the system with a stable potential energy was obtained (Figure S2). The AFICS toolkit was then used to characterize the first coordination sphere of the Cr³⁺ ion within this equilibrated 10 ps trajectory.

As expected, six water molecules coordinate to the Cr3+ ion throughout the AIMD simulation. The results from the AFICS toolkit (Figure 2) report the time-averaged Cr-O distance (the maximum of the first peak in the RDF; Figure 2A) to be 1.98 Å and a maximum threshold distance of 2.22 Å, which is consistent with the 1.96-2.0 Å distances measured experimentally. 70-74 The integral of the RDF (CN) at that threshold distance is 6.0, affirming that there are six waters coordinated and no change in coordination number during the simulation. The angle distribution function (Figure 2B) indicates two peaks at 89 and 175°, which are both near the ideal bond angles (90 and 180°) for an octahedral polyhedron. There are two six-coordinate polyhedra considered by AFICS (octahedral and trigonal prismatic; Figure 1), and the RMSDs of the first ion coordination sphere from each ideal geometry were measured over the course of the trajectory (Figure 2D). The average RMSD between AIMD geometry and the octahedral reference was 0.14 ± 0.032 Å, while the average RMSD compared to the trigonal prismatic reference was 0.76 ± 0.030 Å. The results spotlight the clear preference for the octahedral coordination geometry in the AIMD simulation, confirming the well-known fact that the Cr³⁺ aqua ion is octahedral. What AFICS contributes is in quantifying exactly how octahedral the Cr³⁺ aqua ion is in water at room temperature: 0.14 Å from an ideal octahedron.

AIMD Simulation of the Eu-EDTA Complex. As a demonstration of the AFICS toolkit on a more complex model system, we examined the coordination structure of an aqueous Eu-EDTA complex from a previously reported simulation. S1,81 Identifying the proper coordination structures of solvated Eu and other lanthanide ions remains a challenge as lanthanides have large coordination spheres and predominantly bind to ligands through weaker electrostatic forces instead of orbital interactions. These qualities can allow lanthanide complexes to fluctuate among multiple (sometimes irregular) coordination geometries and vary their coordination number through rapid ligand exchange.

The complete details on the AIMD simulation of aqueous Eu-EDTA may be found in the original article.⁸¹ To summarize the main model features, the Eu³⁺ ion (septet spin state) chelated by unprotonated EDTA (EDTA⁴⁻, the form in basic

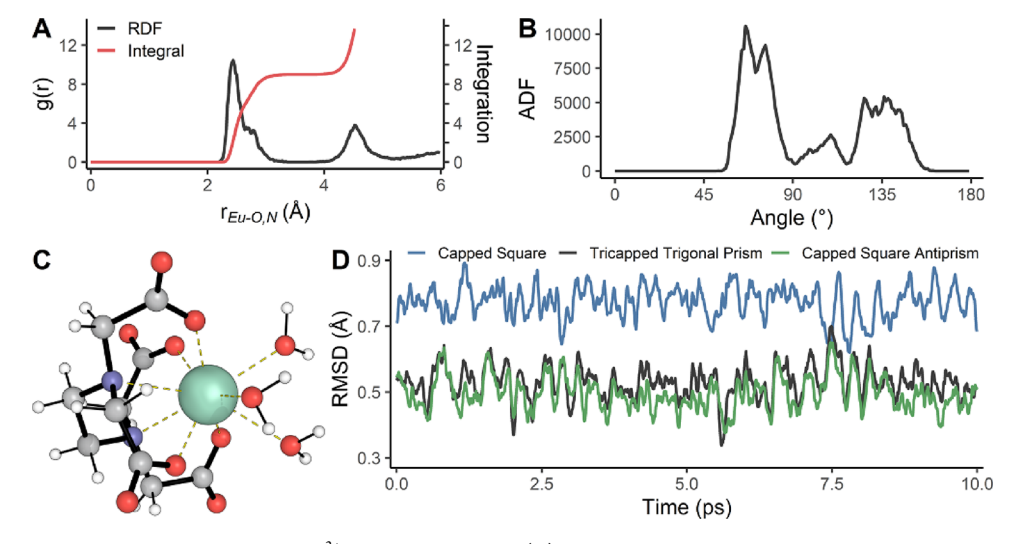


Figure 3. Structural characteristics of the aqueous Eu^{3+} -EDTA simulation: (A) radial distribution function distances of N and O from Eu, (B) angle distribution function formed with Eu^{3+} and surrounding N and O, (C) ball-and-stick model of the first coordination sphere surrounding Eu^{3+} , and (D) deviation of the first ion coordination sphere structure from ideal polyhedral structures over the MD trajectory.

conditions of pH \sim 11) is solvated within a periodic cube (cell length 17.5 Å) by 180 waters and one sodium ion to neutralize the charge of the system. The AIMD simulation was conducted in the NVT ensemble at 298 K until 10 ps of equilibrated trajectory was obtained. The simulation was computed using the same software, method, and level of theory detailed in the previous section for aqueous Cr^{3+} , though with the Eu described by the LnPP1 pseudopotential and basis set. The AFICS toolkit was used to analyze the equilibrated 10 ps trajectory and illustrate the more complicated geometric features of the Eu³⁺ first coordination sphere.

During the simulation, three water molecules are coordinated to the Eu³⁺ along with the two nitrogen and four oxygen atoms of the EDTA ligand, forming a nine-coordinate complex (Figure 3). The inhomogeneity of the coordinating atoms leads to a shoulder in the first peak of the RDF curve (Figure 3A) wherein the principal peak is at 2.44 Å but the ion-atom distances fluctuate up to as much as 3.38 Å for the more weakly bound waters and nitrogen atoms of EDTA. The nonrigid behavior of this system is further exemplified by the broadened peaks observed in the ADF curve shown in Figure 3B. The jagged peaks in the RDF and ADF are a result of the limited sampling inherent with DFT-based MD; classical MD simulations with more extensive sampling would result in smoother peaks. There are three nine-coordinate polyhedra considered by AFICS (capped square, capped square antiprism, and tricapped trigonal prism; Figure 1), and the deviation of the first ion coordination sphere from each ideal geometry over the simulation is presented in Figure 3D. Unlike the Cr3+ hexaaqua structure, which semi-rigidly maintained a structure close to the ideal octahedral geometry, the Eu³⁺-EDTA complex differs more from the ideal geometries and fluctuates among all three shapes. The complex is most frequently arranged in a capped square antiprism geometry with an average RMSD from the ideal reference of 0.50 \pm 0.050 Å, though it will transition to the tricapped trigonal prism geometry (average RMSD of 0.53 \pm 0.050 Å) before returning back to the capped square antiprism geometry. The capped square geometry is only briefly observed during the 10 ps timeframe sampled (average RMSD of $0.77 \pm 0.048 \text{ Å}$).

The shoulder in the RDF (Figure 3A) shows the non-ideal shape of the coordination sphere composed of ligand and solvent molecules. The RMSD values for the Eu-EDTA system, higher than those observed for the Cr³+ aqua ion, are indicative of the deviation from ideal geometries due to an inhomogeneous first coordination sphere. Observing interchanging geometries and structures that are intermediate between two ideal polyhedra is common for systems with polydentate ligands since the geometric constraints imposed by the chelating molecules impose inherent distortions from ideal polyhedra. Despite the changing system, the AFICS toolkit permits users to efficiently measure and differentiate these dynamic structural geometries.

CONCLUSIONS

The AFICS toolkit is a convenient, versatile computational tool for characterizing the geometry of the first coordination sphere surrounding an ion from molecular simulation. AFICS can process the atomic coordinates from a molecular dynamics simulation to identify the coordination structure of an ion and measure how much variation from ideal polyhedra a complex undergoes over time. This tool quantifies information relevant for evaluating structure-property relationships among a variety of systems, particularly those of solvated ions whose structure may be more fluxional or irregular. In this way, the features of AFICS provide a more rigorous technique for gauging the effects that changing ligand design, ion identity, counterion, and solvent choice can have on the ion coordination structure. Lastly, the AFICS tool is not limited toward only analyzing solvated ions; its generalizability may be applied to analyzing other systems not considered in this work, such as the structure of ions within metalloproteins and nanoparticles.

ASSOCIATED CONTENT

Data Availability Statement

The AFICS toolkit and tutorial data are freely available on GitHub: https://github.com/Cantu-Research-Group/AFICS. The version of the code at the time of this publication can also be found in the Supporting Information.

5 Supporting Information

The Supporting Information is available free of charge at https://pubs.acs.org/doi/10.1021/acs.jcim.3c00294.

Figure showing the Cr³⁺ and Eu³⁺-EDTA simulation boxes in atomic resolution; energy plot of the Cr³⁺ simulation; documentation of the AFICS implementation; example code; AFICS Python 3 code (PDF)

AUTHOR INFORMATION

Corresponding Author

David C. Cantu — Department of Chemical and Materials Engineering, University of Nevada, Reno, Reno, Nevada 89557, United States; orcid.org/0000-0001-9584-5062; Email: dcantu@unr.edu

Authors

Stuart J. McElhany – Department of Chemical and Materials Engineering, University of Nevada, Reno, Reno, Nevada 89557, United States

Thomas J. Summers — Department of Chemical and Materials Engineering, University of Nevada, Reno, Reno, Nevada 89557, United States; orcid.org/0000-0002-4243-6078

Richard C. Shiery – Department of Chemical and Materials Engineering, University of Nevada, Reno, Reno, Nevada 89557, United States

Complete contact information is available at: https://pubs.acs.org/10.1021/acs.jcim.3c00294

Notes

The authors declare no competing financial interest.

ACKNOWLEDGMENTS

Support from the National Science Foundation (Award 2041914).

REFERENCES

- (1) Stern, E. A.; Ma, Y.; Hanske-Petitpierre, O.; Bouldin, C. E. Radial Distribution Function in X-Ray-Absorption Fine Structure. *Phys. Rev. B* **1992**, *46*, 687–694.
- (2) Ravel, B.; Kelly, S. D. The Difficult Chore of Measuring Coordination by EXAFS. AIP Conf. Proc. 2007, 882, 150–152.
- (3) Glezakou, V.-A.; Chen, Y.; Fulton, J. L.; Schenter, G. K.; Dang, L. X. Electronic Structure, Statistical Mechanical Simulations, and EXAFS Spectroscopy of Aqueous Potassium. *Theor. Chem. Acc.* **2006**, *115*, 86–99.
- (4) Persson, I. Hydrated Metal Ions in Aqueous Solution: How Regular Are Their Structures? *Pure Appl. Chem.* **2010**, 82, 1901–1917.
- (5) Clark, A. E. Density Functional and Basis Set Dependence of Hydrated Ln(III) Properties. *J. Chem. Theory Comput.* **2008**, *4*, 708–718.
- (6) Yang, T.; Bursten, B. E. Speciation of the Curium(III) Ion in Aqueous Solution: A Combined Study by Quantum Chemistry and Molecular Dynamics Simulation. *Inorg. Chem.* **2006**, *45*, 5291–5301.
- (7) Zhang, J.; Dolg, M. Labile Capping Bonds in Lanthanide(III) Complexes: Shorter and Weaker. J. Phys. Chem. A 2015, 119, 774–780.
- (8) Shor, A. M.; Ivanova-Shor, E. A.; Chiorescu, I.; Krüger, S.; Rösch, N. Hydration Structure and Hydrolysis of U(IV) and Np(IV) Ions: A Comparative Density Functional Study Using a Modified Continuum Solvation Approach. *J. Phys. Chem. A* **2020**, *124*, 3805–3814.
- (9) Kowall, T.; Foglia, F.; Helm, L.; Merbach, A. E. Molecular Dynamics Simulation Study of Lanthanide Ions Ln³⁺ in Aqueous

- Solution Including Water Polarization. Change in Coordination Number from 9 to 8 along the Series. *J. Am. Chem. Soc.* **1995**, 117, 3790–3799.
- (10) Duvail, M.; Vitorge, P.; Spezia, R. Building a Polarizable Pair Interaction Potential for Lanthanoids(III) in Liquid Water: A Molecular Dynamics Study of Structure and Dynamics of the Whole Series. *J. Chem. Phys.* **2009**, 130.
- (11) Marjolin, A.; Gourlaouen, C.; Clavaguera, C.; Ren, P. Y. Y.; Piquemal, J. P.; Dognon, J. P. Hydration Gibbs Free Energies of Open and Closed Shell Trivalent Lanthanide and Actinide Cations from Polarizable Molecular Dynamics. *J. Mol. Model.* **2014**, *20*, 7.
- (12) Chaudhari, M. I.; Soniat, M.; Rempe, S. B. Octa-Coordination and the Aqueous Ba²⁺ Ion. *J. Phys. Chem. B* **2015**, *119*, 8746–8753.
- (13) Qiao, B.; Skanthakumar, S.; Soderholm, L. Comparative CHARMM and AMOEBA Simulations of Lanthanide Hydration Energetics and Experimental Aqueous-Solution Structures. *J. Chem. Theory Comput.* **2018**, *14*, 1781–1790.
- (14) Sessa, F.; D'Angelo, P.; Migliorati, V. Combined Distribution Functions: A Powerful Tool to Identify Cation Coordination Geometries in Liquid Systems. *Chem. Phys. Lett.* **2018**, *691*, 437–443.
- (15) Moll, H.; Denecke, M. A.; Jalilehvand, F.; Sandström, M.; Grenthe, I. Structure of the Aqua Ions and Fluoride Complexes of Uranium(IV) and Thorium(IV) in Aqueous Solution an EXAFS Study. *Inorg. Chem.* **1999**, 38, 1795–1799.
- (16) Allen, P. G.; Bucher, J. J.; Shuh, D. K.; Edelstein, N. M.; Craig, I. Coordination Chemistry of Trivalent Lanthanide and Actinide Ions in Dilute and Concentrated Chloride Solutions. *Inorg. Chem.* **2000**, 39, 595–601.
- (17) Skanthakumar, S.; Antonio, M. R.; Wilson, R. E.; Soderholm, L. The Curium Aqua Ion. *Inorg. Chem.* **2007**, *46*, 3485–3491.
- (18) Persson, I.; D'Angelo, P.; De Panfilis, S.; Sandström, M.; Eriksson, L. Hydration of Lanthanoid(III) Ions in Aqueous Solution and Crystalline Hydrates Studied by EXAFS Spectroscopy and Crystallography: The Myth of the "Gadolinium Break.". *Chem. Eur. J.* **2008**, *14*, 3056–3066.
- (19) De Sio, S. M.; Wilson, R. E. EXAFS Study of the Speciation of Protactinium(V) in Aqueous Hydrofluoric Acid Solutions. *Inorg. Chem.* **2014**, *53*, 12643–12649.
- (20) Ferrier, M. G.; Stein, B. W.; Bone, S. E.; Cary, S. K.; Ditter, A. S.; Kozimor, S. A.; Lezama Pacheco, J. S.; Mocko, V.; Seidler, G. T. The Coordination Chemistry of Cm^{III}, Am^{III}, and Ac^{III} in Nitrate Solutions: An Actinide L₃-Edge EXAFS Study. *Chem. Sci.* **2018**, *9*, 7078–7090.
- (21) Bowron, D. T.; Diaz Moreno, S. Using Synchrotron X-Ray and Neutron Methods to Investigate Structural Aspects of Metal Ion Solvation and Solution Structure: An Approach Using Empirical Potential Structure Refinement. *Coord. Chem. Rev.* **2014**, 277–278, 2–14.
- (22) Palmer, B. J.; Pfund, D. M.; Fulton, J. L. Direct Modeling of EXAFS Spectra from Molecular Dynamics Simulations. *J. Phys* **1996**, *100*, 13393–13398.
- (23) Chillemi, G.; Mancini, G.; Sanna, N.; Barone, V.; Della Longa, S.; Benfatto, M.; Pavel, N. V.; D'Angelo, P. Evidence for Sevenfold Coordination in the First Solvation Shell of Hg(II) Aqua Ion. *J. Am. Chem. Soc.* **2007**, *129*, 5430–5436.
- (24) Fulton, J. L.; Kathmann, S. M.; Schenter, G. K.; Balasubramanian, M. Hydrated Structure of Ag(I) Ion from Symmetry-Dependent, K- and L-Edge XAFS Multiple Scattering and Molecular Dynamics Simulations. *J. Phys. Chem. A* **2009**, *113*, 13976–13984.
- (25) Duvail, M.; D'Angelo, P.; Gaigeot, M. P.; Vitorge, P.; Spezia, R. What First Principles Molecular Dynamics Can Tell Us about EXAFS Spectroscopy of Radioactive Heavy Metal Cations in Water. *Radiochim. Acta* **2009**, *97*, 339–346.
- (26) D'Angelo, P.; Zitolo, A.; Migliorati, V.; Chillemi, G.; Duvail, M.; Vitorge, P.; Abadie, S.; Spezia, R. Revised Ionic Radii of Lanthanoid(III) Ions in Aqueous Solution. *Inorg. Chem.* **2011**, *50*, 4572–4579.

- (27) Fulton, J. L.; Bylaska, E. J.; Bogatko, S.; Balasubramanian, M.; Cauët, E.; Schenter, G. K.; Weare, J. H. Near-Quantitative Agreement of Model-Free DFT-MD Predictions with XAFS Observations of the Hydration Structure of Highly Charged Transition-Metal Ions. *J. Phys. Chem. Lett.* **2012**, *3*, 2588–2593.
- (28) D'Angelo, P.; Martelli, F.; Spezia, R.; Filipponi, A.; Denecke, M. A. Hydration Properties and Ionic Radii of Actinide(III) Ions in Aqueous Solution. *Inorg. Chem.* **2013**, *52*, 10318–10324.
- (29) La Penna, G.; Minicozzi, V.; Morante, S.; Rossi, G. C.; Stellato, F. A First-Principle Calculation of the XANES Spectrum of Cu²⁺ in Water. *J. Chem. Phys.* **2015**, *143*, No. 124508.
- (30) Morales, N.; Galbis, E.; Martínez, J. M.; Pappalardo, R. R.; Sánchez Marcos, E. Identifying Coordination Geometries of Metal Aquaions in Water: Application to the Case of Lanthanoid and Actinoid Hydrates. J. Phys. Chem. Lett. 2016, 7, 4275–4280.
- (31) Pappalardo, R. R.; Caralampio, D. Z.; Martínez, J. M.; Marcos, E. S. Hydration Structure of the Elusive Ac(III) Aqua Ion: Interpretation of X-Ray Absorption Spectroscopy (XAS) Spectra on the Basis of Molecular Dynamics (MD) Simulations. *Inorg. Chem.* **2019**, *58*, 2777–2783.
- (32) Duignan, T. T.; Schenter, G. K.; Fulton, J. L.; Huthwelker, T.; Balasubramanian, M.; Galib, M.; Baer, M. D.; Wilhelm, J.; Hutter, J.; Del Ben, M.; Zhao, X. S.; Mundy, C. J. Quantifying the Hydration Structure of Sodium and Potassium Ions: Taking Additional Steps on Jacob's Ladder. *Phys. Chem. Chem. Phys.* **2020**, 22, 10641–10652.
- (33) Busato, M.; Melchior, A.; Migliorati, V.; Colella, A.; Persson, I.; Mancini, G.; Veclani, D.; D'Angelo, P. Elusive Coordination of the Ag⁺ Ion in Aqueous Solution: Evidence for a Linear Structure. *Inorg. Chem.* **2020**, *59*, 17291–17302.
- (34) Kofod, N.; Nawrocki, P.; Platas-Iglesias, C.; Sørensen, T. J. Electronic Structure of Ytterbium(III) Solvates—a Combined Spectroscopic and Theoretical Study. *Inorg. Chem.* **2021**, *60*, 7453—7464.
- (35) Shiery, R. C.; Fulton, J. L.; Balasubramanian, M.; Nguyen, M.-T.; Lu, J.-B.; Li, J.; Rousseau, R.; Glezakou, V.-A.; Cantu, D. C. Coordination Sphere of Lanthanide Aqua Ions Resolved with Ab Initio Molecular Dynamics and X-Ray Absorption Spectroscopy. *Inorg. Chem.* **2021**, *60*, 3117–3130.
- (36) Driscoll, D. M.; Shiery, R. C.; Balasubramanian, M.; Fulton, J. L.; Cantu, D. C. Ionic Contraction across the Lanthanide Series Decreases the Temperature-Induced Disorder of the Water Coordination Sphere. *Inorg. Chem.* **2022**, *61*, 287–294.
- (37) Driscoll, D. M.; Shiery, R. C.; D'Annunzio, N.; Boglaienko, D.; Balasubramanian, M.; Levitskaia, T. G.; Pearce, C. I.; Govind, N.; Cantu, D. C.; Fulton, J. L. Water Defect Stabilizes the Bi³⁺ Lone-Pair Electronic State Leading to an Unusual Aqueous Hydration Structure. *Inorg. Chem.* **2022**, *61*, 14987–14996.
- (38) Mukherjee, S.; Balius, T. E.; Rizzo, R. C. Docking Validation Resources: Protein Family and Ligand Flexibility Experiments. *J. Chem. Inf. Model.* **2010**, *50*, 1986–2000.
- (39) Bell, E. W.; Zhang, Y. DockRMSD: An Open-Source Tool for Atom Mapping and RMSD Calculation of Symmetric Molecules through Graph Isomorphism. *Aust. J. Chem.* **2019**, *11*, 40.
- (40) Meli, R.; Biggin, P. C. Spyrmsd: Symmetry-Corrected RMSD Calculations in Python. *Aust. J. Chem.* **2020**, *12*, 49.
- (41) Boittier, E. D.; Burns, J. M.; Gandhi, N. S.; Ferro, V. GlycoTorch Vina: Docking Designed and Tested for Glycosaminoglycans. *J. Chem. Inf. Model.* **2020**, *60*, 6328–6343.
- (42) Bao, J.; He, X.; Zhang, J. Z. H. DeepBSP—a Machine Learning Method for Accurate Prediction of Protein—Ligand Docking Structures. J. Chem. Inf. Model. 2021, 61, 2231—2240.
- (43) Caswell, B. T.; de Carvalho, C. C.; Nguyen, H.; Roy, M.; Nguyen, T.; Cantu, D. C. Thioesterase Enzyme Families: Functions, Structures, and Mechanisms. *Protein Sci.* **2022**, *31*, 652–676.
- (44) Durand, S.; Dognon, J. P.; Guilbaud, P.; Rabbe, C.; Wipff, G. Lanthanide and Alkaline-Earth Complexes of EDTA in Water: A Molecular Dynamics Study of Structures and Binding Selectivities. *J. Chem. Soc., Trans.* **2000**, *2*, 705–714.

- (45) McCann, B. W.; De Silva, N.; Windus, T. L.; Gordon, M. S.; Moyer, B. A.; Bryantsev, V. S.; Hay, B. P. Computer-Aided Molecular Design of Bis-Phosphine Oxide Lanthanide Extractants. *Inorg. Chem.* **2016**, *55*, 5787–5803.
- (46) Vo, M. N.; Bryantsev, V. S.; Johnson, J. K.; Keith, J. A. Quantum Chemistry Benchmarking of Binding and Selectivity for Lanthanide Extractants. *Int. J. Quantum Chem.* **2018**, *118*, No. e25516.
- (47) McCarver, G. A.; Hinde, R. J.; Vogiatzis, K. D. Selecting Quantum-Chemical Methods for Lanthanide-Containing Molecules: A Balance between Accuracy and Efficiency. *Inorg. Chem.* **2020**, *59*, 10492–10500.
- (48) Niu, K.; Yang, F.; Gaudin, T.; Ma, H.; Fang, W. Theoretical Study of Effects of Solvents, Ligands, and Anions on Separation of Trivalent Lanthanides and Actinides. *Inorg. Chem.* **2021**, *60*, 9552–9562.
- (49) Regueiro-Figueroa, M.; Esteban-Gómez, D.; de Blas, A.; Rodríguez-Blas, T.; Platas-Iglesias, C. Understanding Stability Trends along the Lanthanide Series. *Chem. Eur. J.* **2014**, *20*, 3974–3981.
- (50) Peterson, C. C.; Penchoff, D. A.; Auxier, J. D.; Hall, H. L. Establishing Cost-Effective Computational Models for the Prediction of Lanthanoid Binding in $[Ln(NO_3)]^{2+}$ (with Ln = La to Lu). ACS Omega 2019, 4, 1375–1385.
- (51) O'Brien, R. D.; Summers, T. J.; Kaliakin, D. S.; Cantu, D. C. The Solution Structures and Relative Stability Constants of Lanthanide–EDTA Complexes Predicted from Computation. *Phys. Chem. Chem. Phys.* **2022**, 24, 10263–10271.
- (52) Vallee, B. L.; Williams, R. J. Metalloenzymes: The Entatic Nature of Their Active Sites. *Proc. Natl. Acad. Sci.* **1968**, *59*, 498–505.
- (53) Karlin, K.; Metalloenzymes, D. Structural Motifs, and Inorganic Models. *Science* **1993**, *261*, 701–708.
- (54) Valdez, C. E.; Smith, Q. A.; Nechay, M. R.; Alexandrova, A. N. Mysteries of Metals in Metalloenzymes. *Acc. Chem. Res.* **2014**, *47*, 3110–3117.
- (55) Boer, J. L.; Mulrooney, S. B.; Hausinger, R. P. Nickel-Dependent Metalloenzymes. *Arch. Biochem. Biophys.* **2014**, 544, 142–152.
- (56) Cotruvo, J. A. J.; Featherston, E. R.; Mattocks, J. A.; Ho, J. V.; Laremore, T. N. Lanmodulin: A Highly Selective Lanthanide-Binding Protein from a Lanthanide-Utilizing Bacterium. *J. Am. Chem. Soc.* **2018**, *140*, 15056–15061.
- (57) Good, N. M.; Fellner, M.; Demirer, K.; Hu, J.; Hausinger, R. P.; Martinez-Gomez, N. C. Lanthanide-Dependent Alcohol Dehydrogenases Require an Essential Aspartate Residue for Metal Coordination and Enzymatic Function. *J. Biol. Chem.* **2020**, 295, 8272–8284.
- (58) Wang, B.; Zhang, X.; Fang, W.; Rovira, C.; Shaik, S. How Do Metalloproteins Tame the Fenton Reaction and Utilize ●OH Radicals in Constructive Manners? *Acc. Chem. Res.* **2022**, *55*, 2280−2290.
- (59) Ketkaew, R.; Tantirungrotechai, Y.; Harding, P.; Chastanet, G.; Guionneau, P.; Marchivie, M.; Harding, D. J. OctaDist: A Tool for Calculating Distortion Parameters in Spin Crossover and Coordination Complexes. *Dalton Trans.* **2021**, *50*, 1086–1096.
- (60) Pinsky, M.; Avnir, D. Continuous Symmetry Measures. 5. The Classical Polyhedra. *Inorg. Chem.* **1998**, *37*, 5575–5582.
- (61) Casanova, D.; Cirera, J.; Llunell, M.; Alemany, P.; Avnir, D.; Alvarez, S. Minimal Distortion Pathways in Polyhedral Rearrangements. J. Am. Chem. Soc. 2004, 126, 1755–1763.
- (62) Cirera, J.; Ruiz, E.; Alvarez, S. Shape and Spin State in Four-Coordinate Transition-Metal Complexes: The Case of the D6 Configuration. *Chem. Eur. J.* **2006**, *12*, 3162–3167.
- (63) van Meel, J. A.; Filion, L.; Valeriani, C.; Frenkel, D. A Parameter-Free, Solid-Angle Based, Nearest-Neighbor Algorithm. *J. Chem. Phys.* **2012**, *136*, No. 234107.
- (64) Staub, R.; Steinmann, S. N. Parameter-Free Coordination Numbers for Solutions and Interfaces. *J. Chem. Phys.* **2020**, *152*, 24124.
- (65) Kepert, D. L. Inorganic Sterochemistry; Springer Verlag, 1982.
- (66) Kepert, D. The Stereochemistry of Eight Coordination. J. Chem. Soc. 1965, 4736–4744.

- (67) Favas, M. C.; Kepert, D. L. Aspects of the Stereochemistry of Four-Coordination and Five-Coordination. In *Progress in Inorganic Chemistry*; John Wiley & Sons, Inc: Hoboken, NJ, USA, 2007; pp. 325–463.
- (68) Ruiz-Martínez, A.; Alvarez, S. Stereochemistry of Compounds with Coordination Number Ten. *Chem. Eur. J.* **2009**, *15*, 7470–7480.
- (69) Kabsch, W. Automatic Processing of Rotation Diffraction Data from Crystals of Initially Unknown Symmetry and Cell Constants. *J. Appl. Crystallogr.* **1993**, 26, 795–800.
- (70) Magini, M. X-ray Diffraction Study of Concentrated Chromium (III) Chloride Solutions. I. Complex Formation Analysis in Equilibrium Conditions. *J. Chem. Phys.* **1980**, *73*, 2499–2505.
- (71) Munoz-Paez, A.; Sanchez Marcos, E. Experimental Evidence by EXAFS of the Second Hydration Shell in Dilute Solutions of Chromium(III) Ion. *J. Am. Chem. Soc.* **1992**, *114*, 6931–6932.
- (72) Díaz-Moreno, S.; Muñoz-Páez, A.; Martínez, J. M.; Pappalardo, R. R.; Marcos, E. S. EXAFS Investigation of Inner- and Outer-Sphere Chloroaquo Complexes of Cr³⁺ in Aqueous Solutions. *J. Am. Chem. Soc.* **1996**, *118*, 12654–12664.
- (73) Lindqvist-Reis, P.; Muñoz-Páez, A.; Díaz-Moreno, S.; Pattanaik, S.; Persson, I.; Sandström, M. The Structure of the Hydrated Gallium(III), Indium(III), and Chromium(III) Ions in Aqueous Solution. A Large Angle X-Ray Scattering and EXAFS Study. *Inorg. Chem.* 1998, 37, 6675–6683.
- (74) Uchikoshi, M.; Akiyama, D.; Kimijima, K.; Shinoda, K. Speciation of Chromium Aqua and Chloro Complexes in Hydrochloric Acid Solutions at 298 K. RSC Adv. 2022, 12, 32722–32736.
- (75) Perdew, J. P.; Burke, K.; Ernzerhof, M. Generalized Gradient Approximation Made Simple. *Phys. Rev. Lett.* **1996**, *77*, 3865–3868.
- (76) Hutter, J.; Iannuzzi, M.; Schiffmann, F.; VandeVondele, J. CP2k: Atomistic Simulations of Condensed Matter Systems. *WIREs Comput. Mol. Sci.* **2014**, *4*, 15–25.
- (77) VandeVondele, J.; Krack, M.; Mohamed, F.; Parrinello, M.; Chassaing, T.; Hutter, J.; Fast, Q. Fast and Accurate Density Functional Calculations Using a Mixed Gaussian and Plane Waves Approach. *Comput. Phys. Commun.* **2005**, *167*, 103–128.
- (78) Goedecker. Separable Dual-Space Gaussian Pseudopotentials. *Phys. Rev. B* **1996**, *54*, 1703–1710.
- (79) VandeVondele, J.; Hutter, J. Gaussian Basis Sets for Accurate Calculations on Molecular Systems in Gas and Condensed Phases. *J. Chem. Phys.* **2007**, *127*, No. 114105.
- (80) Grimme, S.; Antony, J.; Ehrlich, S.; Krieg, H. A Consistent and Accurate Ab Initio Parametrization of Density Functional Dispersion Correction (DFT-D) for the 94 Elements H-Pu. *J. Chem. Phys.* **2010**, 132, No. 154104.
- (81) Kaliakin, D. S.; Sobrinho, J. A.; Monteiro, J. H. S. K.; de Bettencourt-Dias, A.; Cantu, D. C. Solution Structure of a Europium—Nicotianamine Complex Supports That Phytosiderophores Bind Lanthanides. *Phys. Chem. Chem. Phys.* **2021**, 23, 4287–4299.
- (82) Lu, J. B.; Cantu, D. C.; Nguyen, M. T.; Li, J.; Glezakou, V. A.; Rousseau, R. Norm-Conserving Pseudopotentials and Basis Sets to Explore Lanthanide Chemistry in Complex Environments. *J. Chem. Theory Comput.* **2019**, *15*, 5987–5997.

☐ Recommended by ACS

pyCHARMM: Embedding CHARMM Functionality in a Python Framework

Joshua Buckner, Charles L. Brooks III, et al.

JUNE 02, 2023

JOURNAL OF CHEMICAL THEORY AND COMPUTATION

READ 🗹

Consequences of Overfitting the van der Waals Radii of Ions

Madelyn Smith, Pengfei Li, et al.

MARCH 23, 2023

JOURNAL OF CHEMICAL THEORY AND COMPUTATION

READ 🗹

Inclusion of High-Field Target Data in AMOEBA's Calibration Improves Predictions of Protein-Ion Interactions

Julián A. Delgado, Sameer Varma, et al.

SEPTEMBER 29, 2022

JOURNAL OF CHEMICAL INFORMATION AND MODELING

READ 🗹

pDynamo3 Molecular Modeling and Simulation Program

Martin J. Field

NOVEMBER 30, 2022

JOURNAL OF CHEMICAL INFORMATION AND MODELING

READ 🗹

Get More Suggestions >